

GUT MICROBIOTA

Clostridioides difficile uses amino acids associated with gut microbial dysbiosis in a subset of patients with diarrhea

Eric J. Battaglioli^{1*}, Vanessa L. Hale^{2,3*}, Jun Chen⁴, Patricio Jeraldo², Coral Ruiz-Mojica¹, Bradley A. Schmidt¹, Vayu M. Rekdal¹, Lisa M. Till¹, Lutfi Huq², Samuel A. Smits⁵, William J. Moor¹, Yava Jones-Hall⁶, Thomas Smyrk⁷, Sahil Khanna¹, Darrell S. Pardi¹, Madhusudan Grover¹, Robin Patel⁸, Nicholas Chia², Heidi Nelson², Justin L. Sonnenburg⁵, Gianrico Farrugia⁹, Purna C. Kashyap^{1,10†}

The gut microbiota plays a critical role in pathogen defense. Studies using antibiotic-treated mice reveal mechanisms that increase susceptibility to *Clostridioides difficile* infection (CDI), but risk factors associated with CDI in humans extend beyond antibiotic use. Here, we studied the dysbiotic gut microbiota of a subset of patients with diarrhea and modeled the gut microbiota of these patients by fecal transplantation into germ-free mice. When challenged with *C. difficile*, the germ-free mice transplanted with fecal samples from patients with dysbiotic microbial communities showed increased gut amino acid concentrations and greater susceptibility to CDI. A *C. difficile* mutant that was unable to use proline as an energy source was unable to robustly infect germ-free mice transplanted with a dysbiotic or healthy human gut microbiota. Prophylactic dietary intervention using a low-proline or low-protein diet in germ-free mice colonized by a dysbiotic human gut microbiota resulted in decreased expansion of wild-type *C. difficile* after challenge, suggesting that amino acid availability might be important for CDI. Furthermore, a prophylactic fecal microbiota transplant in mice with dysbiosis reduced proline availability and protected the mice from CDI. Last, we identified clinical risk factors that could potentially predict gut microbial dysbiosis and thus greater susceptibility to CDI in a retrospective cohort of patients with diarrhea. Identifying at-risk individuals and reducing their susceptibility to CDI through gut microbiota-targeted therapies could be a new approach to preventing *C. difficile* infection in susceptible patients.

INTRODUCTION

The composition and function of the gut microbiota are integral to the biology of the host. It is well established that a “healthy” gut microbiota is beneficial, whereas a disrupted or dysbiotic microbiota is associated with negative host outcomes including an increased risk of infection, chronic inflammatory or autoimmune conditions, or cancer (1–5). The study of gut microbial dysbiosis as it relates to human health has proved challenging as great variability exists in the composition and function of both healthy and dysbiotic gut microbiotas. It is difficult to assign discrete criteria that ubiquitously define dysbiosis in human populations. To attempt to study gut microbial dysbiosis in a controlled system, mouse models have been developed using antibiotic-mediated perturbations in conventionally raised mice to mimic the human dysbiotic state (6–9). However, limitations include the homogeneous nature of microbial disruption, which fails to capture the diversity of mechanisms that cause gut microbiota alterations

in normal human populations and the inability to mimic the natural and anomalous compositional variations of the human gut microbiota in response to antibiotics or other microbiota-altering insults. A promising alternative is the use of germ-free mice to model the human gut microbiota (10). Recent work has shown that germ-free mice can faithfully recapitulate the structure and function of human gut microbial communities (11, 12).

Diarrhea is one of the most common symptoms of gastrointestinal (GI) disorders, and recent reports have identified gut microbial alterations that are linked to changes in GI transit time (9, 13–15). These diarrhea-induced gut microbial alterations may allow for expansion of opportunistic pathogens. Because diarrhea is a broad symptom reflective of many potential underlying causes of dysbiosis, we examined a patient population with diarrhea to identify human subjects with gut microbial dysbiosis. We then modeled diverse human gut microbial communities in germ-free mice to understand the metabolic and functional changes associated with dysbiosis and their effects on pathogen susceptibility using the common opportunistic gut pathogen *Clostridioides difficile* (formerly *Clostridium difficile*).

C. difficile is considered an opportunistic pathogen due in part to the robust barriers to infection mediated by the gut microbiota. Among these barriers is the microbial production of secondary bile acids, which inhibit *C. difficile* growth (6, 16–18). Disruption of microbial community structure can reduce microbial diversity and production of inhibitory metabolites such as secondary bile acids, creating a permissive condition for *C. difficile* colonization. However, metabolic factors that contribute to successful colonization of *C. difficile* under dysbiotic conditions remain unclear. Here, we

¹Department of Medicine, Division of Gastroenterology and Hepatology, Mayo Clinic, Rochester, MN, USA. ²Department of Surgery, Mayo Clinic, Rochester, MN, USA. ³Department of Veterinary Preventive Medicine, Ohio State University, Columbus, OH, USA. ⁴Department of Health Sciences Research, Mayo Clinic, Rochester, MN, USA. ⁵Department of Microbiology and Immunology, Stanford University, Stanford, CA, USA. ⁶Department of Comparative Pathobiology, Purdue University, West Lafayette, IN, USA. ⁷Department of Laboratory Medicine and Pathology, Division of Anatomic Pathology, Mayo Clinic, Rochester, MN, USA. ⁸Department of Laboratory Medicine and Pathology, Division of Clinical Microbiology, Mayo Clinic, Rochester, MN, USA. ⁹Division of Gastroenterology, Mayo Clinic, Jacksonville, FL, USA. ¹⁰Department of Physiology and Biomedical Engineering, Mayo Clinic, Rochester, MN, USA.

*These authors contributed equally to this work.

†Corresponding author. Email: kashyap.purna@mayo.edu

demonstrate that, when modeled in germ-free mice, the dysbiotic human gut microbiota of patients with diarrhea was characterized by an increase in free amino acids, particularly proline, that rendered the mice more susceptible to *C. difficile* infection.

RESULTS

A subset of patients with diarrhea have a gut microbiota distinct from that of healthy individuals

To determine the effect of diarrhea on the human gut microbiota, we profiled gut microbial community composition using the 16S rRNA gene in 115 patients who presented with diarrhea (table S1). All of the individuals tested negative for *C. difficile* and other common bacterial enteric pathogens and had a spectrum of underlying conditions (e.g., inflammatory bowel disease, irritable bowel syndrome, medication-induced diarrhea, traveler's diarrhea, lactose intolerance, or dysautonomia; fig. S1A). Principal coordinate analysis (PCoA) based on β -diversity showed a wide distribution of microbial communities in the individuals with diarrhea (Fig. 1A). Partitioning around medoids (PAM) clustering analysis with the gap statistic identified two distinct clusters as optimal, a healthy-like cluster (H) and a dysbiotic cluster (D) (Fig. 1A, and fig. S1, B and C) (19).

Microbial communities from patients with diarrhea within the healthy-like cluster grouped with those of 118 healthy controls (20); communities from patients within the dysbiotic cluster did not group with the healthy controls or the healthy-like cluster (Fig. 1, A

and B). In addition, patients within the healthy-like cluster were more likely to be misclassified as healthy controls compared to patients in the dysbiotic cluster based on a random forest supervised learning algorithm using OTU-level abundance (fig. S1D). Hence, we referred to patients within this cluster as healthy-like. Patients within the dysbiotic cluster were referred to as dysbiotic, given the difference in their microbial composition compared to healthy controls. The gut microbiota of the dysbiotic group was characterized by significantly decreased microbial richness and evenness when compared to the gut microbiota of the healthy-like group ($P < 0.0005$; Fig. 1C). In addition, it was characterized by a significantly increased relative abundance of *Enterococcus*, *Enterobacter*, and *Bacteroides* OTUs and decreased *Faecalibacterium*, *Roseburia*, *Blautia*, and *Bacteroides* OTUs ($P < 0.02$; Fig. 1D and table S2) when compared to the gut microbiota of the healthy-like group. Alterations in gut microbial community structure were not associated with a defined etiology of diarrhea ($P = 0.12$, univariable logistic regression; table S3).

To begin to determine the functional consequences of the gut microbial dysbiosis defined above, we compared the community structure of the gut microbiota of dysbiotic individuals to a separate cohort of patients with confirmed *C. difficile* infection (CDI). *C. difficile* is an opportunistic gastrointestinal pathogen of great interest in the clinical setting and has been shown to exploit open niches associated with dysbiosis as a means of establishing infection (2). The dysbiotic gut microbial communities were more similar to the communities

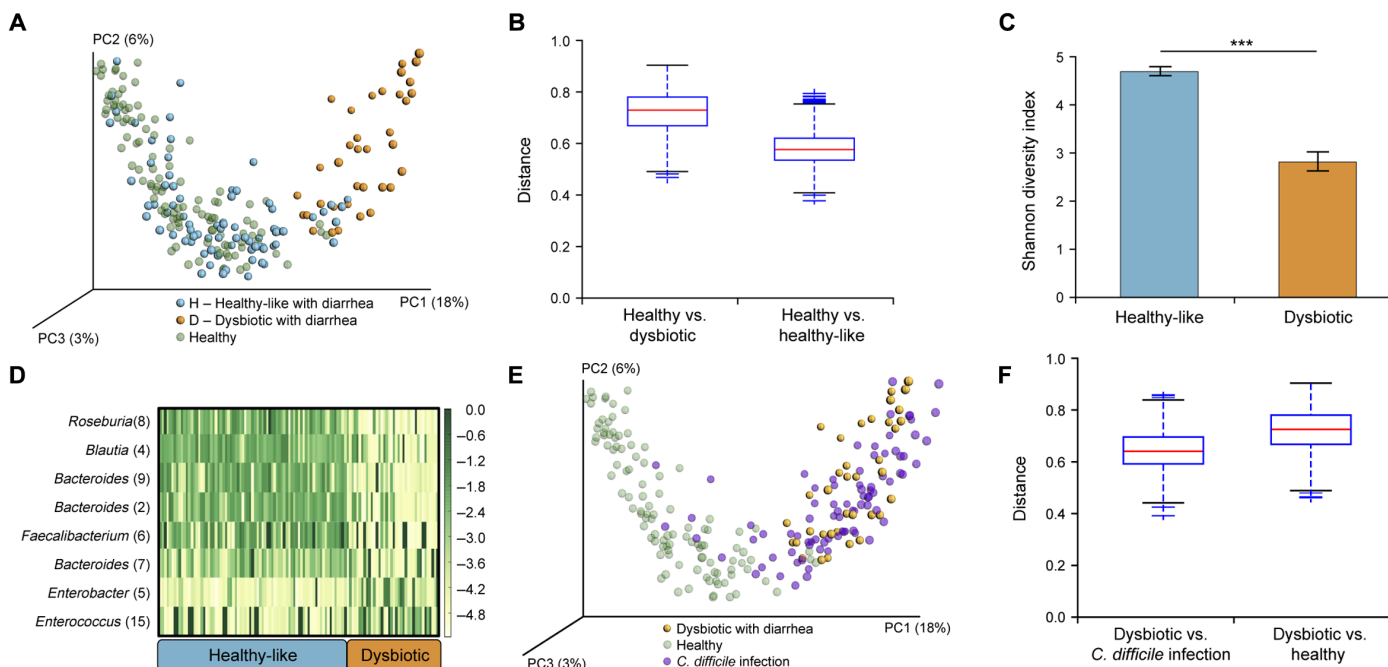


Fig. 1. A subset of patients with diarrhea have a dysbiotic gut microbiota. (A) β -Diversity (unweighted UniFrac) of the gut microbiota of healthy control individuals ($n = 118$) compared to patients with diarrhea clustered on the basis of partitioning around medoids (PAM) [cluster H (healthy-like), $n = 78$ and cluster D (dysbiotic), $n = 37$]. (B) Unweighted UniFrac distances between healthy-like and a dysbiotic gut microbiota from patients with diarrhea compared to a healthy control gut microbiota. The plotted median with interquartile range (IQR) and SD (Bonferroni-corrected $P < 0.0001$, t test) is shown. (C) α -Diversity as indicated by the Shannon diversity index is shown for dysbiotic and healthy-like gut microbiotas from patients with diarrhea. Plotted averages with SEM ($***P < 0.0005$, t test). (D) Heatmap showing significantly different microbial taxa between healthy-like and dysbiotic gut microbial communities. The operational taxonomic unit (OTU) number is featured after the genus (all Bonferroni-corrected $P < 0.02$, Wilcoxon rank-sum test). (E and F) β -Diversity (unweighted UniFrac) of the gut microbiota from (E) healthy control individuals ($n = 118$), dysbiotic patients with diarrhea ($n = 37$), and patients with *C. difficile* infection ($n = 95$); (F) unweighted UniFrac distance between the dysbiotic gut microbiota of patients with diarrhea versus the gut microbiota of healthy controls or those with CDI. Plotted median with IQR and SD (Bonferroni-corrected $P < 0.0001$, t test).

of individuals with confirmed CDI than to those of healthy controls (Fig. 1, E and F). The similarity in structure between the CDI-negative dysbiotic group and the CDI-positive group suggested that CDI-negative dysbiotic communities may display increased susceptibility to CDI and that dysbiosis associated with CDI was not a result of *C. difficile*-mediated remodeling of the community but rather an exploitation of a preformed community-associated phenotype.

A dysbiotic gut microbiota is more susceptible to *C. difficile* infection than a healthy-like gut microbiota

To evaluate community-specific effects on susceptibility to CDI, we modeled human gut microbial communities from representative healthy-like and dysbiotic patients in germ-free mice and challenged them with *C. difficile*. Representative microbial communities from two dysbiotic donors (dysbiotic A and dysbiotic B) and two healthy-like donors (healthy-like A and healthy-like B) were transplanted into germ-free mice (henceforth referred to as dysbiotic and healthy-like mice, respectively), a method previously shown to recapitulate human microbial composition and function (11, 12). The human stool microbial communities were assessed using 16S rRNA gene sequencing after 4 weeks of colonization in germ-free mice, as described previously (12, 21). After colonization, mice clustered based on human donor (representative of the human state), and

UniFrac distances within dysbiotic and healthy-like mouse groups were significantly shorter than distances between dysbiotic and healthy-like mice ($P < 0.0001$; fig. S2A). Similarity to human donor fecal microbiota was 86% at the family level (table S4), which is consistent with previous studies (22). Before *C. difficile* challenge, there was no difference in stool consistency (fig. S2B) or colonic transit time in the transplanted germ-free mice (fig. S2C). In addition, both dysbiotic and healthy-like mice showed normal colon histology with no evidence of inflammation (table S5) and similar amounts of inflammatory cytokines before CDI (fig. S2D). All mice were culture negative for *C. difficile* before challenge.

Dysbiotic and healthy-like mice were challenged with *C. difficile* [$\sim 10^7$ colony-forming units (CFU) per mouse] by oral gavage (fig. S2E). Dysbiotic mice showed significantly higher stool loads of *C. difficile* at day 1 (13.9-fold), day 2 (262-fold), and day 6 compared to healthy-like mice (day 1, $P < 0.00005$; day 2, $P < 0.0005$; day 6, $P < 0.005$). At this point, dysbiotic mice continued to show high *C. difficile* loads, whereas loads were below the limits of detection in healthy-like mice ($P < 0.005$; Fig. 2A). Dysbiotic mice also showed softer stool consistency ($P < 0.0001$; Fig. 2B), increased stool concentrations of *C. difficile* toxin B (Fig. 2C), increased inflammation ($P < 0.0005$; Fig. 2D and table S5), and elevated amounts of CDI-associated cytokines in proximal colon tissue ($P < 0.05$; Fig. 2E) compared

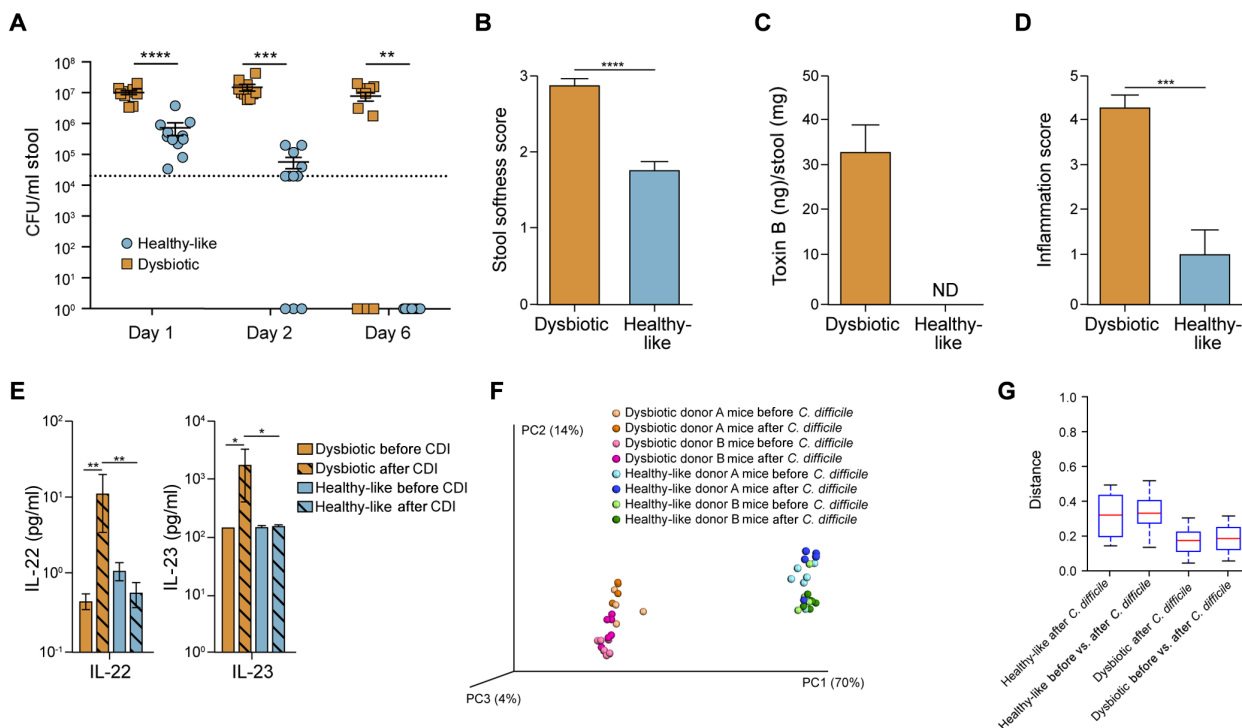


Fig. 2. Mice with a dysbiotic gut microbiota exhibit increased susceptibility to *C. difficile* infection. (A) *C. difficile* CFUs per milliliter of stool from germ-free mice colonized with either a healthy-like ($n = 11$) or dysbiotic ($n = 10$) gut microbiota from patients with diarrhea are shown. Data points represent individual animals with lines indicating average and SEM. Assay limit of detection (LOD) indicated by horizontal dotted line at 2×10^4 CFU/ml stool (** $P < 0.005$, *** $P < 0.0005$, **** $P < 0.00005$, Holm-Šidák test). (B) Stool consistency for germ-free mice transplanted with a healthy-like ($n = 11$) or dysbiotic ($n = 10$) gut microbiota, 2 days after *C. difficile* challenge. Plotted means and SEM (**** $P < 0.0001$, Mann-Whitney test). (C) *C. difficile* toxin B concentrations measured by quantitative ELISA in stool from germ-free mice transplanted with a healthy-like or dysbiotic human gut microbiota, 6 days after *C. difficile* challenge. Plotted means and SEM; ND, not detected. (D) Average proximal colon inflammation score in germ-free mice transplanted with a healthy-like ($n = 11$) or dysbiotic ($n = 10$) human gut microbiota, after *C. difficile* challenge. Plotted means and SEM (**** $P < 0.0005$, Mann-Whitney test). (E) IL-22 and IL-23 concentrations measured from full thickness tissue collected from the proximal colon of germ-free mice transplanted with a dysbiotic ($n = 5$) or healthy-like ($n = 5$) human gut microbiota before and 7 days after *C. difficile* challenge. Plotted means and SEM (* $P < 0.05$, ** $P < 0.005$, Mann-Whitney test). (F) β -Diversity and (G) weighted UniFrac distance comparisons for dysbiotic and healthy-like human gut microbial communities after transplant into germ-free mice before and 2 days after *C. difficile* challenge [Bonferroni-corrected $P = 1$ (dysbiotic), Bonferroni-corrected $P = 1$ (healthy-like), Student's t test].

to healthy-like mice. To determine whether the pathogenesis of *C. difficile* could be attributed to the underlying gut microbial community structure, we compared the gut microbial community composition of dysbiotic and healthy-like mice before and 2 days after *C. difficile* challenge using 16S rRNA sequencing. UniFrac distances within the microbial communities after *C. difficile* challenge were not significantly different from the distance between the microbial communities before and after *C. difficile* challenge ($P = 1$; Fig. 2, F and G, and fig. S2F).

We further validated the CDI susceptibility phenotype observed in the dysbiotic mice using additional technical and biological replicates. We transplanted a new group of germ-free mice with the original dysbiotic and healthy-like fecal samples from A and B donors and challenged these transplanted mice with a separately prepared *C. difficile* inoculum. Similar differences in total bacterial loads, pathology, and toxin production were observed as with the previous dysbiotic and healthy-like mouse A and B cohorts (fig. S3, A to C, and table S5). Further, we assessed the robustness of the phenotype within our healthy-like and dysbiotic mouse A and B cohorts by modeling additional human microbial communities in germ-free mice. Germ-free mice were transplanted with one of eight additional human fecal samples (cohorts C through F)—four healthy-like and four

dysbiotic—and were challenged with *C. difficile*. All groups of dysbiotic mice showed significantly greater stool softness ($P < 0.0005$), toxin production ($P < 0.005$), and inflammation ($P < 0.00005$) when compared with healthy-like communities (fig. S3, D to F). Whereas the *C. difficile* loads in healthy-like mice were lower than those in dysbiotic mice at day 6, the overall *C. difficile* loads were higher in cohorts C to F than those in cohorts A and B, reflecting variability among human donors ($P < 0.005$; fig. S3G).

A dysbiotic gut microbiota has an altered metabolic state characterized by an increase in free amino acids

To characterize the dysbiotic microbial community phenotypes that facilitated susceptibility to CDI, we used transcriptomics and metabolomics to assess community functionality. Whole microbial community gene expression was assessed using RNA-seq on microbial mRNA extracted from the stool of dysbiotic and healthy-like mice. Concurrent metagenomic sequencing was performed on the samples to normalize gene expression based on composition. Pathway analysis using HUMAnN2 (23) showed differences in pathway gene expression among community types. Dysbiotic microbial communities showed significantly decreased expression of multiple genes related to amino acid uptake and metabolism ($P < 0.05$; Fig. 3A). To

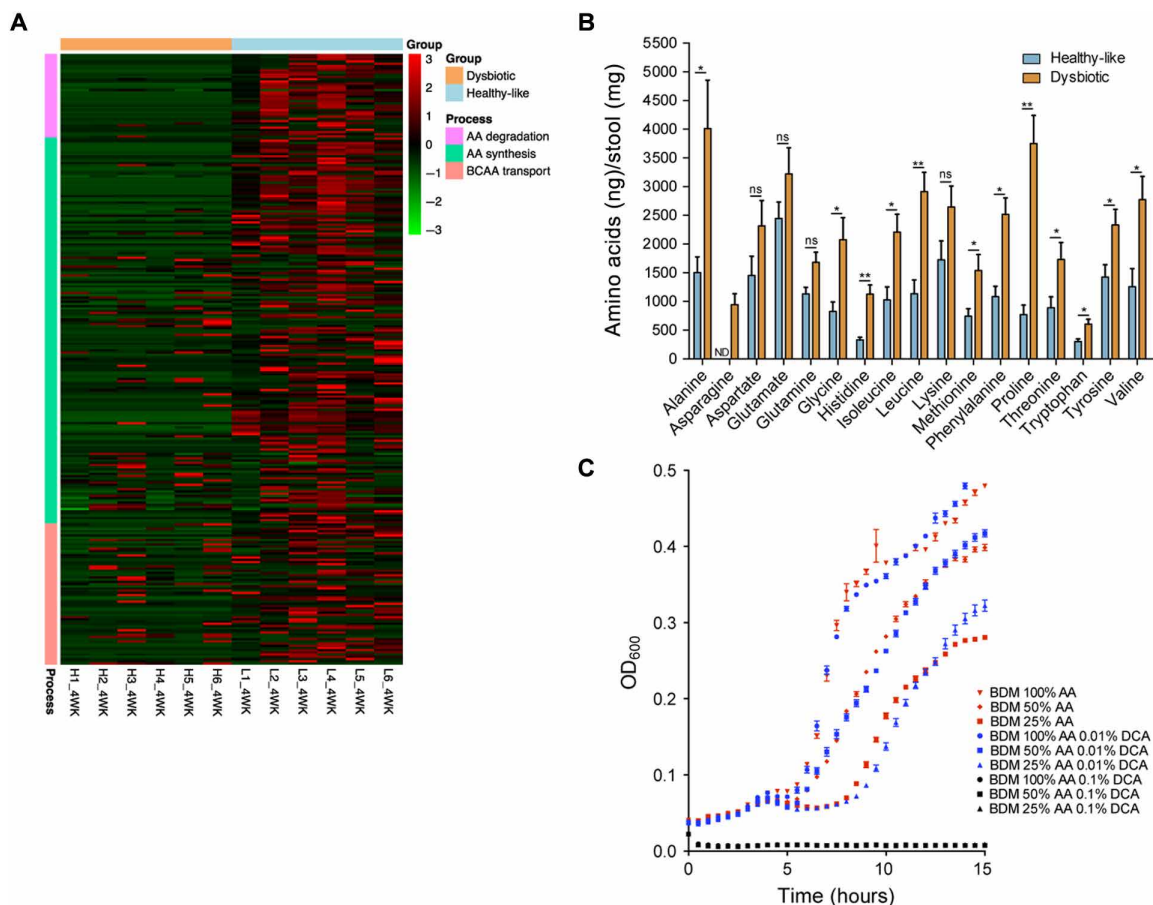


Fig. 3. *C. difficile* exploits increased availability of amino acids in the dysbiotic gut microbiota. (A) A subset of pathway gene expression based on whole gut microbial community gene expression (RNA-seq) normalized using shallow metagenomic sequencing of stool from germ-free mice transplanted with healthy-like ($n = 6$) or dysbiotic ($n = 6$) human gut microbiota before *C. difficile* challenge. (B) Amino acid concentrations in stool from mice transplanted with a healthy-like ($n = 5$) or dysbiotic ($n = 8$) human gut microbiota. Plotted averages and SEM ($*P < 0.05$, $**P < 0.005$, Mann-Whitney test); ns, not significant; ND, not detected. (C) *C. difficile* growth kinetics in basal defined medium (BDM) containing 0, 0.01, or 0.1% deoxycholic acid (DCA) and amino acid concentrations at 100, 50, or 25% of standard media concentrations. Plotted averages and SEM.

determine whether the alterations in gene expression for these amino acid–related pathways had commensurate effects on the overall gut metabolic milieu, we used targeted NMR to quantify amino acids in stool collected from dysbiotic and healthy-like mice before *C. difficile* challenge. Dysbiotic mice showed significantly increased concentrations of 12 amino acids compared to healthy-like mice ($P < 0.05$; Fig. 3B), with proline showing the greatest difference.

Microbial communities in dysbiotic mice also showed reduced gene expression in biosynthetic pathways producing short-chain fatty acids (SCFAs) and secondary bile acids. This was subsequently confirmed using targeted and untargeted metabolomics (fig. S4, A to E, and data files S1 and S2). To determine whether the metabolic state of the dysbiotic mice reflected that of the human donors, we quantified amino acids, SCFAs, and secondary bile acids in stool samples from the original human donors. Human donor fecal samples showed the same differences in amino acid, SCFA, and secondary bile acid concentrations as those observed in the corresponding dysbiotic and healthy-like mice (fig. S5, A to E). These trends were also seen when comparing remaining healthy-like and dysbiotic human fecal samples, which were not used for transplantation experiments (fig. S5, F to J). Similar alterations in SCFA and secondary bile acid concentrations have previously been associated with *C. difficile* susceptibility in antibiotic-treated murine models (6, 8, 24).

Clostridium species are among the best-described users of free amino acids as energy sources (25). Amino acids have been shown to regulate toxin production in vitro (26–29), and recently, they have been predicted to support colonization of *C. difficile* in antibiotic-treated mice (30). However, the effect of amino acid availability on *C. difficile* colonization remains to be elucidated. To examine *C. difficile* reliance on amino acid availability, we assessed in vitro growth kinetics in a defined medium. When grown in basal defined medium with decreasing amino acid concentrations, *C. difficile* showed an amino acid concentration–dependent growth defect in permissive concentrations of deoxycholate (Fig. 3C), suggesting that amino acid availability provided a distinct growth advantage under permissive, low secondary bile acid conditions.

The ability to utilize proline provides a competitive advantage to *C. difficile* in dysbiotic mice

To further assess whether amino acids provided a competitive advantage to *C. difficile*, we analyzed the role of proline, which was the most differentially abundant amino acid between the healthy-like and dysbiotic mice (Fig. 3B). *C. difficile* is capable of using proline as a sole energy source via Stickland fermentation (26, 27, 31). In addition, other strains of *C. difficile* have been shown to be auxotrophic for proline, and this was confirmed for our *C. difficile* 630 isolate (Fig. 4A). Microbial RNA-seq gene expression profiles from dysbiotic and healthy-like mice revealed increased expression of *prdA*, one of the essential enzymatic components in Stickland fermentation, in healthy-like mice before *C. difficile* challenge (Fig. 4B). After *C. difficile* challenge, *prdA* expression was detected in both healthy-like and dysbiotic mice (Table 1). However, in healthy-like mice, *prdA* expression was attributed to three commensal bacteria—*Clostridium hylemonae*, *Dorea longicatena*, and *Lachnospiraceae bacterium 5_1_57FAA*—whereas, in dysbiotic mice, *prdA* expression was exclusively attributed to *C. difficile*. This suggested that *C. difficile* was readily able to scavenge and use free proline in the dysbiotic gut microbiota. Despite the presence of *C. difficile* in healthy-like mice at the time of sampling (day 2), no *C. difficile*–specific *prdA* gene

expression was detected, suggesting that *C. difficile* was unable to compete for free proline in healthy-like mice.

To determine the relevance of proline for *C. difficile* colonization in vivo, we examined colonization and pathogenesis of a *prdB* mutant variant of *C. difficile* 630 in the dysbiotic and healthy-like mice (27). PrdB is one of the essential enzymes in the proline Stickland fermentation pathway, and the *prdB* mutant is unable to use proline as an energy source (27). After challenge with the *C. difficile prdB* mutant, analysis showed reduced colonization and *C. difficile* toxin B concentrations compared to wild-type *C. difficile* in dysbiotic mice (Fig. 4, C and D). In addition, the *prdB* mutant was undetectable in healthy-like mice at day 1 after challenge, whereas wild-type *C. difficile* remained detectable through day 2 after challenge (Fig. 4C).

The attenuation of the *prdB C. difficile* mutant suggested that proline availability was an important factor governing colonization of *C. difficile* in germ-free mice transplanted with fecal samples from healthy-like and dysbiotic individuals. To test whether manipulating proline availability in the gut could restore protection to a susceptible dysbiotic gut microbiota, germ-free mice were transitioned from standard chow to custom isocaloric diets with or without proline and then were transplanted with human dysbiotic fecal samples and challenged with *C. difficile* (fig. S6A and table S6). Dysbiotic mice fed a proline-deficient diet showed a fivefold decrease in *C. difficile* loads at day 1 after *C. difficile* challenge (fig. S6B), suggesting that proline availability alone could affect early expansion of *C. difficile*. To determine whether amino acids other than proline played a role in this process, we performed a similar experiment using a standard [19% (w/v)] or custom isocaloric diet with reduced [2% (w/v)] protein content (fig. S6C and table S6). Dysbiotic mice fed the reduced protein diet showed a 10-fold decrease in *C. difficile* load at day 1 after challenge (fig. S6D), suggesting that, whereas proline is an important contributor, the availability of other amino acids may also influence early expansion of *C. difficile* in a dysbiotic gut microbial community.

Gut microbiota–targeted therapy for CDI reduces free proline and decreases CDI susceptibility in dysbiotic mice

The predominant non-antibiotic microbiota-targeted therapy for CDI is fecal microbiota transplant (FMT). To determine whether FMT could reduce *C. difficile* susceptibility in dysbiotic mice, we delivered a mouse-adapted healthy human–derived FMT gut microbial community to dysbiotic and healthy-like mice (fig. S7A). 16S rRNA analysis revealed a significant shift in the gut microbial communities of dysbiotic mice to resemble the human fecal donor community after FMT ($P < 0.0001$; Fig. 5, A and B). The gut microbiota of healthy-like mice was relatively unaltered by FMT (fig. S7B). There was a significant increase in microbial richness and evenness after FMT in dysbiotic mice ($P < 0.0005$; Fig. 5C). FMT-treated dysbiotic mice became resistant to CDI and showed no detectable *C. difficile* in stool at day 1, 2, or 6 after *C. difficile* challenge; they showed normal colon histology at day 7 after challenge (fig. S7, C and D). We examined proline availability before and after FMT in dysbiotic mice using NMR and found a significant decrease in free proline after FMT ($P < 0.005$; Fig. 5D), supporting a role for proline in the susceptibility of dysbiotic mice to *C. difficile* challenge. FMT-treated dysbiotic mice also showed an increased abundance of SCFAs and secondary bile acids (fig. S7, E and F) as previously reported, suggesting a normalization of the overall gut metabolic milieu to a more healthy state. The concentration of SCFAs and secondary bile acids in healthy-like mice remained unchanged after FMT (fig. S7, G and H).

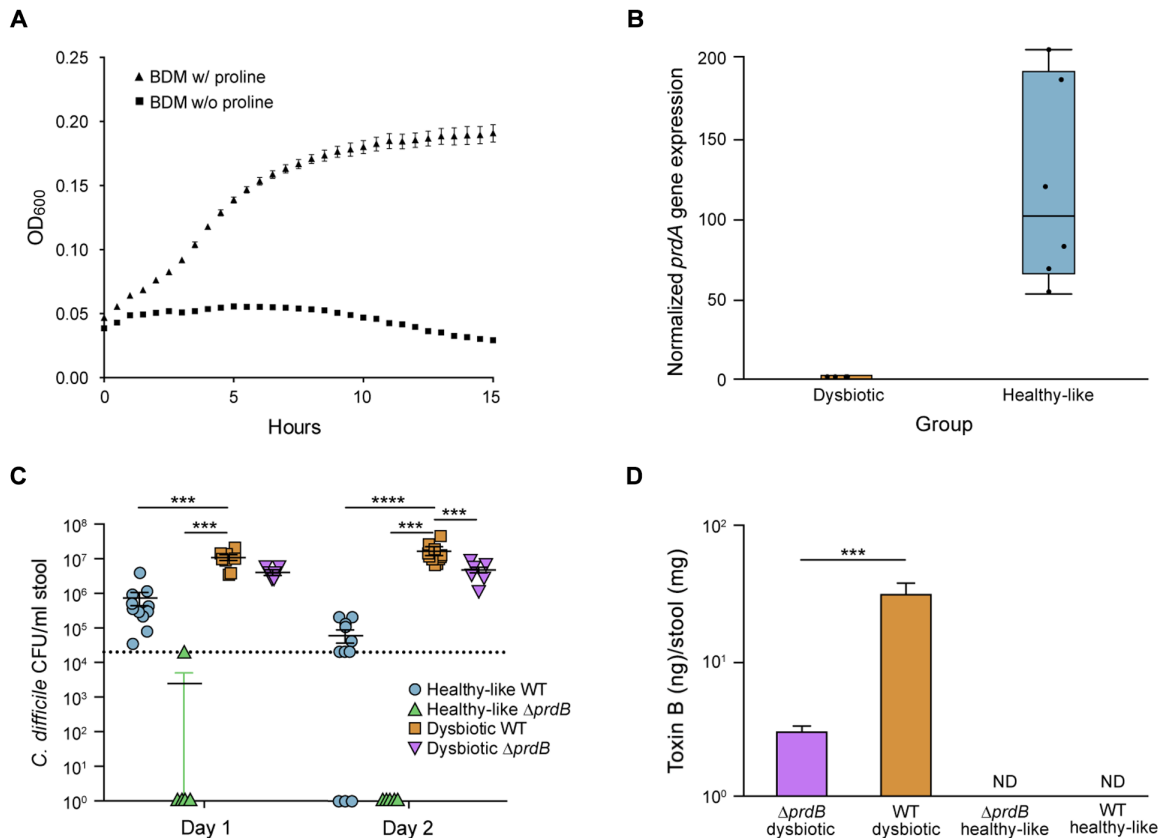


Fig. 4. Proline affects *C. difficile* colonization in germ-free mice transplanted with a dysbiotic or healthy-like human gut microbiota. (A) *C. difficile* growth kinetics indicated optical density (OD) at 600 nm in the presence or absence of proline in basal defined medium without glucose. Plotted means and SEM. (B) D-proline reductase A (*prdA*) expression normalized to metagenomic read counts in the healthy-like and dysbiotic gut microbiota of transplanted mice before *C. difficile* challenge. (C) Δ *prdB* mutant *C. difficile* CFU/ml stool from germ-free mice transplanted with a dysbiotic ($n = 7$) or healthy-like ($n = 8$) human gut microbiota after *C. difficile* challenge is shown. Colonization of the transplanted mice with wild-type (WT) *C. difficile* from Fig. 2A is also shown. Data points represent individual animals with lines indicating average and SEM. Assay limit of detection (LOD) indicated by a horizontal dotted line at 2×10^4 CFU/ml stool ($***P < 0.005$, $****P < 0.0005$, two-way ANOVA). (D) *C. difficile* toxin B concentrations were measured by quantitative ELISA in the stool of mice transplanted with a dysbiotic ($n = 7$) or a healthy-like ($n = 8$) human gut microbiota 6 days after challenge with Δ *prdB* mutant *C. difficile* or wild-type *C. difficile* (data from Fig. 2C). Plotted means and SEM ($***P < 0.0005$, Mann-Whitney test).

Table 1. Absolute counts of *prdA* gene expression in dysbiotic and healthy-like mice at day 2 after *C. difficile* challenge by taxonomic group.

Mouse ID	Dysbiotic						Healthy-like					
	M1	M2	M3	M4	M5	M6	M1	M2	M3	M4	M5	M6
<i>Clostridium difficile</i>	5314	5100	3798	1823	5774	2764	0	0	0	0	0	0
<i>Clostridium hylemonae</i>	0	0	0	0	0	0	518	0	0	412	460	0
<i>Dorea longicatena</i>	0	0	0	0	0	0	4678	0	2171	0	0	0
<i>Lachnospiraceae bacterium 5_1_57FAA</i>	0	0	0	0	0	0	0	0	1266	0	3425	0

Five clinical features can be used to predict individuals with gut microbiota dysbiosis who might be at risk for CDI

The use of dietary interventions and FMT as prophylactic microbiota-targeted therapies in at-risk individuals represents a new strategy for reducing the incidence of CDI. However, implementation of such therapies is conditional on identifying at-risk individuals in the clinical setting. We examined clinical metadata associated with the healthy-

like and dysbiotic patients described in Fig. 1A to identify clinical features that may predict gut microbial dysbiosis. Five clinical features (potential risk factors) predicted dysbiosis in these patients: antibiotic use within the previous 3 weeks (odds ratio, 95% confidence interval, P value: OR, 5.21; 95% CI, 2.14 to 12.71; $P < 0.001$), immunosuppression (OR, 2.87; 95% CI, 1.27 to 6.48; $P = 0.012$), current hospitalization (OR, 6.17; 95% CI, 2.22 to 17.15; $P < 0.001$), recent hospitalization

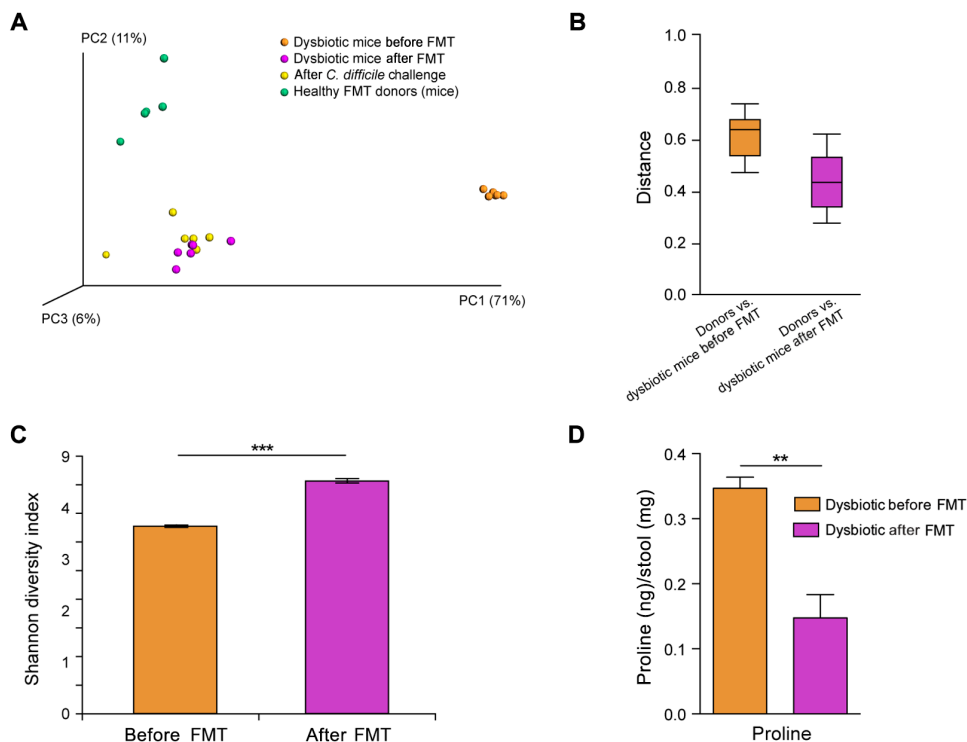


Fig. 5. Fecal microbiota transplant from healthy individuals reduces free proline and susceptibility of transplanted mice to *C. difficile* infection. (A) β -Diversity (weighted UniFrac) of mice transplanted with a dysbiotic human gut microbiota, before and after a fecal microbiota transplant (FMT) from healthy individuals ($n = 6$). (B) Distances (weighted UniFrac) between FMT healthy donors and mice transplanted with a dysbiotic gut microbiota were significantly decreased after FMT (Bonferroni-corrected $P < 0.0001$, Student's t test). (C) α -Diversity of the dysbiotic gut microbiota in transplanted mice before and after FMT ($n = 6$). Plotted averages and SEM (** $P < 0.0005$, Student's t test). (D) Proline concentrations in stool from mice transplanted with a dysbiotic gut microbiota, before and after FMT ($n = 6$). Plotted averages and SEM (** $P < 0.005$, Mann-Whitney test).

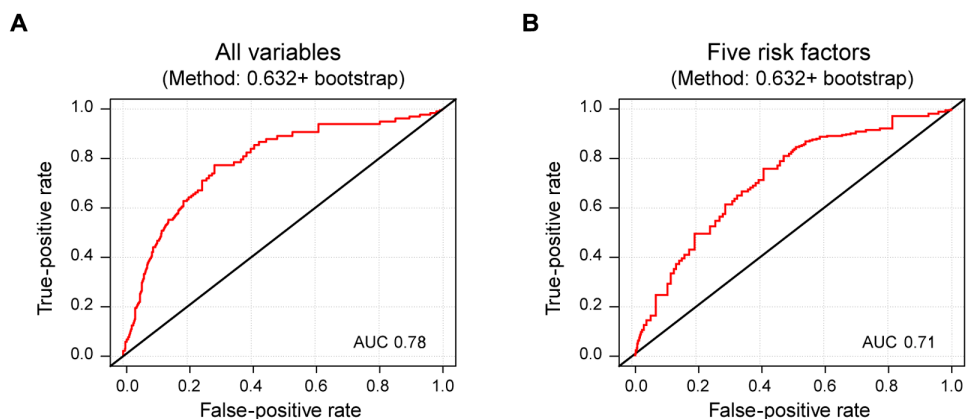


Fig. 6. Five clinical risk factors may predict gut microbial dysbiosis and susceptibility to *C. difficile* infection in patients with diarrhea. (A) Receiver operating characteristic (ROC) curve based on five clinical risk factors that may be predictive of gut microbiota dysbiosis. Recent antibiotics (OR, 5.21; 95% CI, 2.14 to 12.71; $P < 0.001$), immunosuppression (OR, 2.87; 95% CI, 1.27 to 6.48; $P = 0.012$), current hospitalization (OR, 6.17; 95% CI, 2.22 to 17.15; $P < 0.001$), recent hospitalization (OR, 4.87; 95% CI, 1.72 to 13.74; $P = 0.003$), and prior *C. difficile* infection (OR, 9.26; 95% CI, 2.37 to 36.20; $P = 0.001$). Area under the curve (AUC), 0.78 (see table S4). (B) ROC curve based on five clinical risk factors that may be predictive of *C. difficile* infection. Recent antibiotics (OR, 3.35; 95% CI, 2.78 to 4.03; $P = 6.21 \times 10^{-37}$), immunosuppression (OR, 2.47; 95% CI, 2.06 to 2.96; $P = 8.42 \times 10^{-23}$), current hospitalization (OR, 2.94; 95% CI, 2.40 to 3.61; $P = 8.45 \times 10^{-25}$), recent hospitalization (OR, 3.32; 95% CI, 2.72 to 4.06; $P = 1.85 \times 10^{-31}$), and prior *C. difficile* infection (OR, 5.84; 95% CI, 4.42 to 7.72; $P = 1.66 \times 10^{-35}$). AUC, 0.71.

(OR, 4.87; 95% CI, 1.72 to 13.74; $P = 0.003$), and prior CDI (OR, 9.26; 95% CI, 2.37 to 36.20; $P = 0.001$; fig. S8, A to E, and table S7). Age, sex, and body mass index were not significantly associated with dysbiosis ($P \geq 0.05$; table S7). Patients within the dysbiotic group exhibited a significantly greater number of potential risk factors compared to healthy-like individuals [dysbiotic: mean, 1.97 risk factors per person (SD, 1.19); healthy-like: mean, 0.64 risk factors per person (SD, 0.93); $P < 10^{-8}$, Wilcoxon rank-sum test). These five clinical features were predictors of dysbiosis based on receiver operating characteristic (ROC) curve analysis [area under the curve (AUC), 0.78; Fig. 6A].

In our germ-free mouse model, dysbiosis was associated with increased susceptibility to CDI. To determine whether the five clinical features that were predictive of dysbiosis were also predictive of CDI in patients with diarrhea, we examined the electronic medical records of a retrospective cohort of consecutive patients with diarrhea between June 2012 and September 2015. All patients underwent stool testing; for those found to be negative for CDI, their medical records ($n = 17,190$) were included in the study. As a single patient may have had multiple tests, the first negative test was considered to be the index visit; hence, the total number is reflective of unique patients. We then examined electronic medical records to assess individual risk factors in this population including prior history of *C. difficile* infection (within 12 months of the index visit, average time between prior CDI diagnosis and index visit was 91 days, median was 51 days, and range was 3 to 359 days), recent hospitalization (within the previous 4 weeks), current hospitalization and antibiotic use (within the previous 3 weeks), and immunosuppression, as well as subsequent episodes of CDI after index visit. The electronic medical records for 17,190 patients showed that 493 patients subsequently developed CDI (average time between index visit and positive CDI diagnosis was 81 days, median was 46 days, and range was 1 to 364 days; Table 2). Each of the risk factors was a significant predictor of CDI, with odds ratios ranging from 2.47 to 5.84, based on univariable logistic regression ($P < 10^{-22}$; Table 3). Multivariable logistic regression with ROC curve analysis confirmed that the five potential risk factors combined were also strong predictors

Table 2. Demographics of patients who developed *C. difficile* infection after initially testing negative.

	Developed CDI (n = 493)	Did not developed CDI (n = 16,697)	P value
Sex, n (%)			
Male	252 (51)	7391 (44)	0.003
Female	241 (49)	9306 (56)	
Age (year)			
Mean (SD)	56.8 (17.7)	57.1 (18.6)	0.726
Range	18–95	18–106	
BMI			
Mean (SD)	29 (17.7)	28 (7.3)	0.002
Range	14–79	10–100	

Table 3. Risk factors predictive of *C. difficile* infection.

Risk factor	Odds ratio (95% CI)	P value
Antibiotics	3.35 (2.78–4.03)	6.2×10^{-37}
Immunosuppression	2.47 (2.06–2.96)	8.4×10^{-23}
Recent hospitalization	3.32 (2.72–4.06)	1.8×10^{-31}
Current hospitalization	2.94 (2.40–3.61)	8.4×10^{-25}
Prior CDI	5.84 (4.42–7.72)	1.6×10^{-35}
Any one risk factor	1.16 (0.74–1.83)	0.51
Any two risk factors	3.89 (2.76–5.48)	7.4×10^{-15}
Any three risk factors	5.00 (3.59–6.96)	1.2×10^{-21}
Any four risk factors	9.28 (6.67–12.91)	5.4×10^{-40}
All five risk factors	24.24 (12.96–45.32)	1.8×10^{-23}

of CDI (AUC, 0.71; Fig. 6B). In addition, the odds of developing CDI were 24 times higher when comparing those without any risk factors to those with the five potential risk factors (Table 3).

DISCUSSION

Here, we demonstrate that a subset of patients with diarrhea had a gut microbial community structure that was distinct from that of healthy controls and was independent of disease etiology. The dysbiotic gut microbiota of patients with diarrhea was characterized by an increase in free amino acids, especially proline, and showed increased susceptibility to *C. difficile* infection after transplant into germ-free mice. Resistance to *C. difficile* colonization, however, was restored after prophylactic FMT from a healthy donor into mice previously transplanted with a dysbiotic human gut microbiota from patients with diarrhea. A *C. difficile* *prdB* mutant which cannot use proline as an energy source showed attenuated growth in germ-free mice transplanted with either a dysbiotic or a healthy-like human gut microbiota, indicating that amino acids, such as proline, may be an important nutritional niche that can be exploited by *C. difficile*. In addition, we identified simple clinical metrics that potentially could be used to identify patients with a dysbiotic gut microbiota and, consequently, an increased risk of *C. difficile* infection.

Current rodent models of gut dysbiosis-associated pathogen susceptibility have used antibiotics to induce gut dysbiosis before pathogen exposure (24, 32, 33). This type of dysbiosis is homogeneous and is not reflective of the composition or diversity of human dysbiotic gut microbial communities, thus limiting the translatability of these models. In this study, we demonstrate susceptibility to *C. difficile* infection using native human gut microbial communities transplanted into germ-free mice that were not subjected to antibiotic treatment. The ability to model non-antibiotic factors underlying human gut microbial dysbiosis is important, given the increase in non-antibiotic-associated *C. difficile* infections (34–37). Our approach can be applied to assess susceptibility to infection of other dysbiosis-associated enteric pathogens including *Escherichia coli*, *Salmonella* spp., and *Enterococcus* spp. (38).

Our results demonstrate that the metabolic milieu generated by gut microbial dysbiosis creates a complex environment that can regulate both colonization and pathogenicity of *C. difficile*. The lack of

change in gut microbial community composition after exposure to *C. difficile* in transplanted germ-free mice suggested that the susceptibility phenotype is an underlying characteristic of the microbial community rather than a *C. difficile*-mediated event. The nutrient niche hypothesis (39–42) posits that colonization resistance is maximized in microbial communities, where commensal microbes efficiently use all available nutrients. The relative abundance of free amino acids in a dysbiotic compared to a healthy-like gut microbiota suggests that suboptimal nutrient utilization may be a consequence of dysbiosis. Although concentrations of free amino acids varied among individuals with a dysbiotic gut microbiota, the relative abundance of proline and the lack of inhibitory secondary bile acids (6, 16–18, 43) created a unique niche, which *C. difficile* readily occupied. Furthermore, recent studies have shown that fecal amino acids positively correlated with the severity of Crohn's disease (44). This indicates that increased amino acid availability may be an important mechanistic effector in certain gut microbial dysbiosis-related pathologies.

The attenuation of growth of a *C. difficile* *prdB* mutant, which cannot use proline as an energy source, suggests that proline availability affects the fitness of *C. difficile*. *C. difficile* is also a proline auxotroph (29, 45), and in a proline-restricted environment, *C. difficile* fitness is suppressed. This is supported by the accelerated clearance and reduced load of a *C. difficile* *prdB* mutant compared to wild-type *C. difficile* observed in mice transplanted with a healthy-like or dysbiotic gut microbiota. The rapid clearance of the mutant strain in mice transplanted with a healthy-like gut microbiota supports the role of proline in *C. difficile* colonization. The attenuated growth rather than rapid clearance of the *prdB* mutant strain in mice with a dysbiotic gut microbiota may be attributed to the availability of alternative amino acids, which were also increased because of dysbiosis. Whereas our study provides evidence supporting the role of proline in susceptibility to *C. difficile* infection, it is likely that proline is not the sole determinant of *C. difficile* pathogenesis. The relative roles of individual and combinations of amino acids elevated in dysbiotic microbial communities and the effects of proline and other amino acids on regulating the production of *C. difficile* toxins and eliciting host responses will need to be assessed in future studies.

Dietary proline is not essential for humans (46), and protein-based dietary interventions are partially protective in animal models of *C. difficile* infection (47), suggesting that a proline-deficient diet

could be a simple actionable therapy for providing protection to at-risk individuals. However, several nondietary factors regulate the concentration of free amino acids in the colon. Thus, using a combination of defined microbial communities that could act as amino acid scavengers or FMT in conjunction with dietary interventions could be effective for preventing *C. difficile* infection in at-risk individuals.

Analysis of the clinical metadata associated with the patient cohort in the current study revealed five risk factors, readily available in electronic medical records, that may be predictive of gut microbial dysbiosis. Further, in a retrospective cohort of 17,190 patients who presented with diarrhea, these five risk factors were associated with *C. difficile* infection.

There are several limitations to our study. Our mouse model was able to capture the biological variability in the gut microbial communities from different individuals. However, individual-specific mechanisms of these gut microbial communities will still need to be examined using a combination of multi-omic sequencing, in vitro techniques, and gnotobiotic mouse models transplanted with a defined consortium of bacterial species. Here, we focused on the model laboratory strain *C. difficile* 630; however, there are differences in colonization and host responses among different *C. difficile* clinical isolates. Future studies investigating the effect of proline utilization by different strains of *C. difficile*, the effect of proline on toxin production by individual isolates, and the effects of different *C. difficile* strains on mice carrying a healthy-like or dysbiotic gut microbiota will further clarify the role of proline in strain-specific outcomes. In addition, the virome and fungome were not evaluated in this study but may have a role in influencing *C. difficile* susceptibility and should be evaluated in future studies. We identified potential clinical features associated with dysbiosis in our study that were also associated with a risk of future *C. difficile* infection. These will need to be further validated in additional patient cohorts across different centers. Our findings set the stage for future prospective human studies aimed at preventing *C. difficile* infection using dietary and microbiota-targeted therapies to correct gut microbial dysbiosis as a strategy to reduce the incidence of *C. difficile* infection.

MATERIALS AND METHODS

Study design

This study was designed to assess the effects of diarrhea-associated gut microbiota dysbiosis and underlying mechanisms associated with it which increased susceptibility to *C. difficile* infection in transplanted germ-free mice. This was assessed by (i) identifying individuals with diarrhea who had a dysbiotic microbial community structure using 16S rRNA sequencing, (ii) assessing the effects of diarrhea-associated dysbiosis on susceptibility to *C. difficile* infection in germ-free mice transplanted with a dysbiotic gut microbiota, (iii) characterizing gut metabolites that were associated with dysbiosis and susceptibility to *C. difficile* infection, (iv) evaluating the ability of *C. difficile* to use specific metabolites present in the dysbiotic microbial communities in vitro and in vivo, and (v) analyzing clinical data to look for associations of medical features with gut microbial dysbiosis and *C. difficile* infection.

Human studies

The Mayo Clinic Institutional Review Board approved all human studies. Adults (>18 years old) who presented with diarrhea and tested negative for *C. difficile* and other common bacterial sources

of diarrhea ($n = 115$; IRB no. 12-007176) and those who tested positive for *C. difficile* detected by PCR ($n = 95$; IRB no. 12-000554) (48) were voluntarily enrolled. Upon receiving consent from participants, frozen stool leftover from clinical testing was obtained and stored at -80°C until DNA extraction. Participants were recruited at Mayo Clinic in Rochester, MN. The healthy control group ($n = 118$) comprised volunteers who provided stool samples to the Midwest Reference Range Biobank (IRB no. 13-003694) (20).

Animal studies

Animal experiments were performed with germ-free Swiss Webster mice born and maintained in the Mayo Clinic Germ-Free Mouse Facility as described previously (49). *C. difficile* susceptibility was assessed using sex-matched, germ-free mice. Sample sizes were chosen on the basis of similar prior studies (12, 22, 50) and logistical constraints within gnotobiotic isolators. Littermates were used when possible to minimize contamination risks associated with multiple germ-free transfers; however, formal randomization was not used. Germ-free animal technicians performed mouse allocation, and investigators were blinded to selection. *C. difficile* colonization and infection were assessed by stool colony-forming units, toxin concentration, and histology. All mouse experiments complied with Institutional Animal Care and Use Committee guidelines (IACUC protocol no. A32015). Two representative dysbiotic or healthy-like human gut microbial communities were used to assess susceptibility to infection; an additional four representative communities from each group were evaluated to assess reproducibility of associated phenotypes.

C. difficile challenge in transplanted germ-free mice

Germ-free mice were transplanted with stool suspensions prepared from patients in the human “dysbiotic” and “healthy-like” groups. A total of 59 4-week-old mice were transplanted with dysbiotic A stool ($n = 4$), dysbiotic B stool ($n = 6$), dysbiotic C stool ($n = 8$), dysbiotic D stool ($n = 5$), dysbiotic E stool ($n = 4$), dysbiotic F stool ($n = 4$), healthy-like A stool ($n = 5$), healthy-like B stool ($n = 6$), healthy-like C stool ($n = 4$), healthy-like D stool ($n = 5$), healthy-like E stool ($n = 4$), or healthy-like F stool ($n = 4$). Mice transplanted with the same human samples were cohoused in covered cages separated by sex. Communities A/B and E/F from each group were cohoused within isolators, whereas communities C and D were housed in separate isolators.

Human-derived gut microbial communities were allowed 4 weeks to adapt to the mouse gut after transplantation. The transplanted mice then were challenged by oral gavage with $\sim 10^7$ CFU of either *C. difficile* strain 630 or a $\Delta prdB$ mutant strain. Fecal pellets were collected before *C. difficile* challenge and at days 1, 2, and 6 after *C. difficile* challenge for analyses of *C. difficile* colony counts, 16S rRNA community analysis, and metabolomics (fig. S2E). Stool consistency was evaluated using the following stool softness scoring system: 1 = hard, dry pellets, difficult to transect with a disposable plastic culture loop; 2 = soft, fully formed pellets, easy to transect with a culture loop; and 3 = runny, poorly formed pellets, no pressure required to transect with a culture loop. Whole gut transit time was assessed using carmine red as described previously (15). Mice were euthanized on day 7, and proximal colon tissue samples were collected at necropsy. Colon contents were removed, and the tissue was rinsed with Krebs solution with mannitol (115 mM NaCl, 2 mM KH_2PO_4 , 2.4 mM $\text{MgCl}_2 \cdot 6\text{H}_2\text{O}$, 25 mM NaHCO_3 , 8 mM KCl, 1.3 mM CaCl_2 , and 250 mM mannitol). A 5 mm by 5 mm section of proximal colon tissue

was stored in 10% formalin for paraffin embedding and hematoxylin and eosin (H&E) staining.

The ability of dietary intervention to provide protection against *C. difficile* challenge was assessed using the germ-free mouse model (fig. S6, A to C). Germ-free mice were transitioned to one of three custom diets: a low (2%) protein diet that was nutrient-matched and isocaloric to standard 5K67 mouse chow (D16062104, Research Diets), a defined control diet (A16062101, Research Diets), or a defined control diet that was proline deficient (A16062102, Research Diets; table S6). After 4 days of the custom diets, mice were transplanted with dysbiotic mouse stool (originating from dysbiotic A or dysbiotic B human donors). A total of 15 4-week-old mice ($n = 5$ per diet) were transplanted, and 4 weeks later, mice were challenged with *C. difficile*. Pellets were collected at days 1, 2, and 6 after *C. difficile* challenge for *C. difficile* colony counts, 16S rRNA community analysis, and metabolomics. Mice were euthanized on day 7 after *C. difficile* challenge, and colon tissue samples were collected at necropsy as described above.

The ability of prophylactic FMT to confer resistance to *C. difficile* challenge was also assessed in the germ-free mouse model (fig. S7A). Fecal suspensions were generated by suspending frozen mouse pellets collected 4 weeks after transplantation of mice with dysbiotic A or dysbiotic B stool from the *C. difficile* susceptibility experiment. A total of 12 4-week-old mice received fecal suspensions via oral gavage from dysbiotic A ($n = 3$), dysbiotic B ($n = 3$), healthy-like A ($n = 3$), or healthy-like B ($n = 3$) and were housed, as described above. Four weeks after colonization, mice were given two FMT 4 days apart. FMTs were prepared by combining six freshly collected mouse pellets from mice previously transplanted with stool from a healthy human donor mixed 1:1 with prerduced 1× PBS. Suspension (300 μ l) was administered to each mouse via oral gavage. One week after the FMT, the mice were challenged with *C. difficile* as described above. Fecal pellets were collected from the mice before and after FMT and on days 1, 2, and 6 after *C. difficile* challenge for *C. difficile* colony counts, 16S rRNA community analysis, and metabolomics. Mice were euthanized on day 7 after *C. difficile* challenge, and colon tissue samples were collected at necropsy as described above.

C. difficile colonization and toxin production

One pellet was used to quantify *C. difficile* stool load at days 1, 2, and 6 after *C. difficile* challenge. A 1- μ l aliquot of each fecal pellet was measured by filling the opening in a 1- μ l sterile inoculation loop and suspending it in sterile prerduced PBS. The resulting suspension was serially diluted in duplicate, spotted onto prerduced CDMN agar medium, and incubated anaerobically at 37°C for 24 hours. Identifiable *C. difficile* colonies were counted, and CFU per milliliter of stool were calculated. The concentration of *C. difficile* toxin B in stool was assessed by ELISA (tgcBIOMICS) according to the manufacturer's instructions and was normalized to stool mass.

Clinical risk factor analysis

In the first patient cohort of 115 individuals with diarrhea who tested negative for *C. difficile* (IRB no. 12-007176), electronic medical records were examined, and univariable logistic regression (R-3.1.2) was used to examine potential risk factors for dysbiosis including demographic features (age, sex, and BMI) and clinical features. Odds ratios were calculated for each risk factor. Odds ratios for number of risk factors per patient were also calculated in relation to the baseline group (0 risk factors). The 0.632+ bootstrap method (51)

based on multivariable logistic regression was then used to generate an ROC curve with the five clinical features predictive of dysbiosis (antibiotic use within the previous 3 weeks, immunosuppression, current hospitalization, recent hospitalization within the previous 4 weeks, and prior *C. difficile* infection).

The same five clinical risk factors were evaluated in a retrospective cohort of 17,190 patients who presented with diarrhea but all tested negative for *C. difficile*. To obtain this cohort, we first examined all *C. difficile* test records ($n = 39,629$) at Mayo Clinic, Rochester, MN between November 2011 and April 2016 (IRB no. 16-003622). We then selected all patients who tested negative for *C. difficile* between June 2012 and September 2015, providing a 7-month window of *C. difficile* test data on either side of our selected date range to evaluate prior and future *C. difficile* infection incidence. For patients tested more than once during the selected date range, the first negative test was identified as the index visit ($n = 17,190$ unique patients). As described above, univariable and multivariable logistic regression was run on demographic and clinical risk factors to determine whether these risk factors predicted *C. difficile* infection (if a patient tested positive for *C. difficile* infection multiple times after the index visit, only the first positive *C. difficile* test date after the index visit was recorded). Odds ratios were also calculated as above for risk factors and number of risk factors in relation to *C. difficile* infection. For prior *C. difficile* infection, only positive *C. difficile* tests within 12 months of the index date were included in the analyses. The ROC curve was based on bootstrapping (500 times) to counter potential overfitting.

Statistical analysis

Analyses for 16S rRNA sequence data were performed in QIIME 1.9.1, R-3.1.2, and SAS 9.3. Partitioning around medoids (PAM) clustering performed in R-3.1.2 was used to define clusters in human patient samples. Optimal cluster number was determined by the gap statistic and confirmed by the ASW (average silhouette width) statistic based on unweighted UniFrac distances (19, 52). Shannon diversity indices (assessing microbial abundance and evenness) were calculated in QIIME and compared using *t* tests in Microsoft Excel. Relative abundances of microbial taxa were compared between groups by Kruskal-Wallis tests. Differences in UniFrac-based β -diversity metrics were assessed using PERMANOVA. Random forests (supervised_learning.py) and distance analyses (make_distance_boxplots.py) were also run in QIIME to classify and determine similarities between groups. RNA-seq differential expression analysis was performed using DESeq2 v. 1.8.2 (53), with a *P* value cutoff of $P < 0.05$, and using LefSe (54) for pathway significance analysis for normalized RNA-seq data. Untargeted metabolomics PCoA analyses were performed by using \log_2 peak fold change, and *P* values were calculated with Kruskal-Wallis *H* tests. Statistical analyses for *C. difficile* colonization, toxin concentrations, histological scores, host cytokine expression, and targeted metabolite concentrations were performed with GraphPad Prism Software, version 6.0. Data are presented as means \pm SEM, and statistical comparisons were assessed using non-parametric tests. Single-pair analyses were performed by a Mann-Whitney test, and multivariable comparison by Holm-Sidak and two-way ANOVA with a *P* value cutoff of $P < 0.05$, as indicated in the figure legends. A univariable logistic regression model was used to calculate the odds ratio and the significance of individual clinical risk factors. An ROC curve was constructed using 0.632+ bootstrap method (51) based on a multivariable logistic regression model. Cluster analysis, logistic regression, and ROC analysis were performed in R-3.1.2.

SUPPLEMENTARY MATERIALS

www.sciencetranslationalmedicine.org/cgi/content/full/10/464/eaam7019/DC1

Materials and Methods

Fig. S1. Etiology and cluster analysis of patients with diarrhea.

Fig. S2. Microbial community and host phenotypes of healthy-like and dysbiotic mice.

Fig. S3. Technical and biological replication of healthy-like and dysbiotic microbial communities.

Fig. S4. Metatranscriptomics and metabolomics indicate that SCFAs and secondary bile acids inhibit *C. difficile* colonization.

Fig. S5. Metabolic properties of healthy-like and dysbiotic human stool samples.

Fig. S6. Dietary intervention reduces early *C. difficile* colonization in dysbiotic mice.

Fig. S7. FMT decreases susceptibility to CDI and normalizes the metabolic milieu.

Fig. S8. Distribution of healthy-like and dysbiotic individuals by risk factors that are predictive of dysbiosis.

Table S1. Patient cohort demographics.

Table S2. Taxonomic differences between healthy-like and dysbiotic individuals.

Table S3. Etiology of diarrhea by community type.

Table S4. Efficiency of transfer of human gut microbiota to mice at the family level.

Table S5. Colon inflammation scores.

Table S6. Custom diet formulations.

Table S7. Demographics and risk factors predictive of dysbiosis.

Data file S1. Untargeted metabolomics with metabolites increased in healthy-like mice.

Data file S2. Untargeted metabolomics with metabolites increased in dysbiotic mice.

Data file S3. Source data for main figures and tables.

Data file S4. Source data for supplementary figures and tables.

References (55–62)

REFERENCES AND NOTES

- M. D. Schulz, C. Atay, J. Heringer, F. K. Romrig, S. Schwitala, B. Aydin, P. K. Ziegler, J. Varga, W. Reindl, C. Pommerenke, G. Salinas-Riester, A. Böck, C. Alpert, M. Blaut, S. C. Polson, L. Brandl, T. Kirchner, F. R. Greten, S. W. Polson, M. C. Arkan, High-fat-diet-mediated dysbiosis promotes intestinal carcinogenesis independently of obesity. *Nature* **514**, 508–512 (2014).
- R. A. Britton, V. B. Young, Role of the intestinal microbiota in resistance to colonization by *Clostridium difficile*. *Gastroenterology* **146**, 1547–1553 (2014).
- Y. Maeda, T. Kurakawa, E. Umamoto, D. Motooka, Y. Ito, K. Gotoh, K. Hirota, M. Matsushita, Y. Furuta, M. Narazaki, N. Sakaguchi, H. Kayama, S. Nakamura, T. Iida, Y. Saeki, A. Kumanogoh, S. Sakaguchi, K. Takeda, Dysbiosis contributes to arthritis development via activation of autoreactive T cells in the intestine. *Arthritis Rheumatol.* **68**, 2646–2661 (2016).
- M. Rajilic-Stojanovic, D. M. Jonkers, A. Salonen, K. Hanevik, J. Raes, J. Jalanka, W. M. de Vos, C. Manichanh, N. Golic, P. Enck, E. Philippou, F. A. Iraqi, G. Clarke, R. C. Spiller, J. Penders, Intestinal microbiota and diet in IBS: Causes, consequences, or epiphenomena? *Am. J. Gastroenterol.* **110**, 278–287 (2015).
- K. M. Keeney, S. Yurist-Doutsch, M. C. Arrieta, B. B. Finlay, Effects of antibiotics on human microbiome and subsequent disease. *Annu. Rev. Microbiol.* **68**, 217–235 (2014).
- C. G. Buffie, V. Bucci, R. R. Stein, P. T. McKenney, L. Ling, A. Gobourne, D. No, H. Liu, M. Kinnebrew, A. Viale, E. Littmann, M. R. M. van den Brink, R. R. Jenq, Y. Taur, C. Sander, J. R. Cross, N. C. Toussaint, J. B. Xavier, E. G. Pamer, Precision microbiome reconstitution restores bile acid mediated resistance to *Clostridium difficile*. *Nature* **517**, 205–208 (2015).
- K. M. Ng, J. A. Ferreyra, S. K. Higginbottom, J. B. Lynch, P. C. Kashyap, S. Gopinath, N. Naidu, B. Choudhury, B. C. Weimer, D. M. Monack, J. L. Sonnenburg, Microbiota-liberated host sugars facilitate post-antibiotic expansion of enteric pathogens. *Nature* **502**, 96–99 (2013).
- C. M. Theriot, M. J. Koenigsnecht, P. E. Carlson Jr., G. E. Hatton, A. M. Nelson, B. Li, G. B. Huffnagle, J. Z. Li, V. B. Young, Antibiotic-induced shifts in the mouse gut microbiome and metabolome increase susceptibility to *Clostridium difficile* infection. *Nat. Commun.* **5**, 3114 (2014).
- J. A. Ferreyra, K. J. Wu, A. J. Hryckowian, D. M. Bouley, B. C. Weimer, J. L. Sonnenburg, Gut microbiota-produced succinate promotes *C. difficile* infection after antibiotic treatment or motility disturbance. *Cell Host Microbe* **16**, 770–777 (2014).
- J. Collins, J. M. Auchtung, L. Schaefer, K. A. Eaton, R. A. Britton, Humanized microbiota mice as a model of recurrent *Clostridium difficile* disease. *Microbiome* **3**, 35 (2015).
- A. Marcobal, P. C. Kashyap, T. A. Nelson, P. A. Aronov, M. S. Donia, A. Spormann, M. A. Fischbach, J. L. Sonnenburg, A metabolomic view of how the human gut microbiota impacts the host metabolome using humanized and gnotobiotic mice. *ISME J.* **7**, 1933–1943 (2013).
- P. J. Turnbaugh, V. K. Ridaura, J. J. Faith, F. E. Rey, R. Knight, J. I. Gordon, The effect of diet on the human gut microbiome: A metagenomic analysis in humanized gnotobiotic mice. *Sci. Transl. Med.* **1**, 6ra14 (2009).
- D. Vandeputte, G. Falony, S. Vieira-Silva, R. Y. Tito, M. Joossens, J. Raes, Stool consistency is strongly associated with gut microbiota richness and composition, enterotypes and bacterial growth rates. *Gut* **65**, 57–62 (2016).
- H. M. Roager, L. B. S. Hansen, M. I. Bahl, H. L. Frandsen, V. Carvalho, R. J. Gøbel, M. D. Dalgaard, D. R. Plichta, M. H. Sparholt, H. Vestergaard, T. Hansen, T. Sicheritz-Pontén, H. B. Nielsen, O. Pedersen, L. Lauritzen, M. Kristensen, R. Gupta, T. R. Licht, Colonic transit time is related to bacterial metabolism and mucosal turnover in the gut. *Nat. Microbiol.* **1**, 16093 (2016).
- P. C. Kashyap, A. Marcobal, L. K. Ursell, M. Larauche, H. Duboc, K. A. Earle, E. D. Sonnenburg, J. A. Ferreyra, S. K. Higginbottom, M. Million, Y. Tache, P. J. Pasricha, R. Knight, G. Farrugia, J. L. Sonnenburg, Complex interactions among diet, gastrointestinal transit, and gut microbiota in humanized mice. *Gastroenterology* **144**, 967–977 (2013).
- J. A. Sorg, A. L. Sonenshein, Inhibiting the initiation of *Clostridium difficile* spore germination using analogs of chenodeoxycholic acid, a bile acid. *J. Bacteriol.* **192**, 4983–4990 (2010).
- J. A. Sorg, A. L. Sonenshein, Bile salts and glycine as cogerminants for *Clostridium difficile* spores. *J. Bacteriol.* **190**, 2505–2512 (2008).
- J. A. Sorg, A. L. Sonenshein, Chenodeoxycholate is an inhibitor of *Clostridium difficile* spore germination. *J. Bacteriol.* **191**, 1115–1117 (2009).
- R. Tibshirani, G. Walther, T. Hastie, Estimating the number of clusters in a data set via the gap statistic. *J. R. Stat. Soc. B* **63**, 411–423 (2001).
- J. Chen, E. Ryu, M. Hathcock, K. Ballman, N. Chia, J. E. Olson, H. Nelson, Impact of demographics on human gut microbial diversity in a US Midwest population. *PeerJ* **4**, e1514 (2016).
- C. R. Kelly, S. Kahn, P. Kashyap, L. Laine, D. Rubin, A. Atreja, T. Moore, G. Wu, Update on fecal microbiota transplantation 2015: Indications, methodologies, mechanisms, and outlook. *Gastroenterology* **149**, 223–237 (2015).
- V. K. Ridaura, J. J. Faith, F. E. Rey, J. Cheng, A. E. Duncan, A. L. Kau, N. W. Griffin, V. Lombard, B. Henrissat, J. R. Bain, M. J. Muehlbauer, O. Ilkayeva, C. F. Semenkovich, K. Funai, D. K. Hayashi, B. J. Lyle, M. C. Martini, L. K. Ursell, J. C. Clemente, W. Van Treuren, W. A. Walters, R. Knight, C. B. Newgard, A. C. Heath, J. I. Gordon, Gut microbiota from twins discordant for obesity modulate metabolism in mice. *Science* **341**, 1241214 (2013).
- S. Abubucker, N. Segata, J. Goll, A. M. Schubert, J. Izard, B. L. Cantarel, B. Rodriguez-Mueller, J. Zucker, M. Thiagarajan, B. Henrissat, O. White, S. T. Kelley, B. Methé, P. D. Schloss, D. Gevers, M. Mitreva, C. Huttenhower, Metabolic reconstruction for metagenomic data and its application to the human microbiome. *PLoS Comput. Biol.* **8**, e1002358 (2012).
- C. M. Theriot, A. A. Bowman, V. B. Young, Antibiotic-induced alterations of the gut microbiota alter secondary bile acid production and allow for *Clostridium difficile* spore germination and outgrowth in the large intestine. *mSphere* **1**, e00045-15 (2016).
- Z. L. Dai, G. Wu, W. Y. Zhu, Amino acid metabolism in intestinal bacteria: Links between gut ecology and host health. *Front Biosci.* **16**, 1768–1786 (2011).
- L. Bouillaut, T. Dubois, A. L. Sonenshein, B. Dupuy, Integration of metabolism and virulence in *Clostridium difficile*. *Res Microbiol.* **166**, 375–383 (2015).
- L. Bouillaut, W. T. Self, A. L. Sonenshein, Proline-dependent regulation of *Clostridium difficile* Stickland metabolism. *J. Bacteriol.* **195**, 844–854 (2013).
- M. Neumann-Schaal, J. D. Hofmann, S. E. Will, D. Schomburg, Time-resolved amino acid uptake of *Clostridium difficile* 630Δerm and concomitant fermentation product and toxin formation. *BMC Microbiol.* **15**, 281 (2015).
- K. Yamakawa, S. Kamiya, X. Q. Meng, T. Karasawa, S. Nakamura, Toxin production by *Clostridium difficile* in a defined medium with limited amino acids. *J. Med. Microbiol.* **41**, 319–323 (1994).
- M. L. Jenior, J. L. Leslie, V. B. Young, P. D. Schloss, *Clostridium difficile* colonizes alternative nutrient niches during infection across distinct murine gut microbiomes. *mSystems* **2**, e00063-17 (2017).
- S. Jackson, M. Calos, A. Myers, W. T. Self, Analysis of proline reduction in the nosocomial pathogen *Clostridium difficile*. *J. Bacteriol.* **188**, 8487–8495 (2006).
- M. Wlodarska, B. Willing, K. M. Keeney, A. Menendez, K. S. Bergstrom, N. Gill, S. L. Russell, B. A. Vallance, B. B. Finlay, Antibiotic treatment alters the colonic mucus layer and predisposes the host to exacerbated *Citrobacter rodentium*-induced colitis. *Infect. Immun.* **79**, 1536–1545 (2011).
- J. P. Zackular, J. L. Moore, A. T. Jordan, L. J. Juttukonda, M. J. Noto, M. R. Nicholson, J. D. Crews, M. W. Semler, Y. Zhang, L. B. Ware, M. K. Washington, W. J. Chazin, R. M. Caprioli, E. P. Skaar, Dietary zinc alters the microbiota and decreases resistance to *Clostridium difficile* infection. *Nat Med.* **22**, 1330–1334 (2016).
- H. Pituch, *Clostridium difficile* is no longer just a nosocomial infection or an infection of adults. *Int. J. Antimicrob. Agents* **33** (suppl. 1), S42–S45 (2009).
- S. S. Kwon, J. L. Gim, M. S. Kim, H. Kim, J. Y. Choi, D. Yong, K. Lee, Clinical and molecular characteristics of community-acquired *Clostridium difficile* infections in comparison with those of hospital-acquired *C. difficile*. *Anaerobe* **48**, 42–46 (2017).

36. S. Khanna, D. S. Pardi, The growing incidence and severity of *Clostridium difficile* infection in inpatient and outpatient settings. *Expert. Rev. Gastroenterol Hepatol.* **4**, 409–416 (2010).
37. S. Khanna, D. S. Pardi, S. L. Aronson, P. P. Kammer, R. Orenstein, J. L. St Sauver, W. S. Harmsen, A. R. Zinsmeister, The epidemiology of community-acquired *Clostridium difficile* infection: A population-based study. *Am. J. Gastroenterol.* **107**, 89–95 (2012).
38. B. Stecher, The roles of inflammation, nutrient availability and the commensal microbiota in enteric pathogen infection. *Microbiol. Spectr.* **3**, 10.1128/microbiolspec.MBP-0008-2014 (2015).
39. A. M. Schubert, M. A. M. Rogers, C. Ring, J. Mogle, J. P. Petrosino, V. B. Young, D. M. Aronoff, P. D. Schloss, Microbiome data distinguish patients with *Clostridium difficile* infection and non-*C. difficile*-associated diarrhea from healthy controls. *MBio* **5**, e01021-14 (2014).
40. G. P. Donaldson, S. M. Lee, S. K. Mazmanian, Gut biogeography of the bacterial microbiota. *Nat. Rev. Microbiol.* **14**, 20–32 (2016).
41. R. Freter, H. Brickner, M. Botney, D. Cleven, A. Aranki, Mechanisms that control bacterial populations in continuous-flow culture models of mouse large intestinal flora. *Infect. Immun.* **39**, 676–685. (1983).
42. K. H. Wilson, F. Perini, Role of competition for nutrients in suppression of *Clostridium difficile* by the colonic microflora. *Infect. Immun.* **56**, 2610–2614 (1988).
43. B. Stecher, D. Berry, A. Loy, Colonization resistance and microbial ecophysiology: Using gnotobiotic mouse models and single-cell technology to explore the intestinal jungle. *FEMS Microbiol. Rev.* **37**, 793–829 (2013).
44. J. L. Giel, J. A. Sorg, A. L. Sonenshein, J. Zhu, Metabolism of bile salts in mice influences spore germination in *Clostridium difficile*. *PLoS ONE* **5**, e8740 (2010).
45. J. Ni, T.-C. D. Shen, E. Z. Chen, K. Bittinger, A. Bailey, M. Roggiani, A. Sirota-Madi, E. S. Friedman, L. Chau, A. Lin, I. Nissim, J. Scott, A. Lauder, C. Hoffmann, G. Rivas, L. Albenberg, R. N. Baldassano, J. Braun, R. J. Xavier, C. B. Clish, M. Yudkoff, H. Li, M. Goulian, F. D. Bushman, J. D. Lewis, G. D. Wu, A role for bacterial urease in gut dysbiosis and Crohn's disease. *Sci. Transl. Med.* **9**, eaah6888 (2017).
46. T. Karasawa, S. Ikoma, K. Yamakawa, S. Nakamura, A defined growth medium for *Clostridium difficile*. *Microbiology* **141**, 371–375 (1995).
47. P. Trumbo, S. Schlicker, A. A. Yates, M. Poos; Food, and Nutrition Board of the Institute of Medicine, The National Academies, Dietary reference intakes for energy, carbohydrate, fiber, fat, fatty acids, cholesterol, protein and amino acids. *J. Am. Diet. Assoc.* **102**, 1621–1630 (2002).
48. L. M. Sloan, B. J. Duresko, D. R. Gustafson, J. E. Rosenblatt, Comparison of real-time PCR for detection of the *tcdC* gene with four toxin immunoassays and culture in diagnosis of *Clostridium difficile* infection. *J. Clin. Microbiol.* **46**, 1996–2001 (2008).
49. C. S. Reigstad, C. E. Salmonson, J. F. Rainey III, J. H. Szurszewski, D. R. Linden, P. L. Sonnenburg, G. Farrugia, P. C. Kashyap, Gut microbes promote colonic serotonin production through an effect of short-chain fatty acids on enterochromaffin cells. *FASEB J.* **29**, 1395–1403 (2015).
50. F. Bäckhed, J. K. Manchester, C. F. Semenkovich, J. I. Gordon, Mechanisms underlying the resistance to diet-induced obesity in germ-free mice. *Proc. Natl. Acad. Sci. U.S.A.* **104**, 979–984 (2007).
51. B. Efron, R. Tibshirani, Improvements on cross-validation: The .632 bootstrap method. *J. Am. Stat. Assoc.* **92**, 548–560 (1997).
52. P. J. Rousseeuw, Silhouettes: A graphical aid to the interpretation and validation of cluster-analysis. *J. Comput. Appl. Math.* **20**, 53–65 (1987).
53. M. I. Love, W. Huber, S. Anders, Moderated estimation of fold change and dispersion for RNA-seq data with DESeq2. *Genome Biol.* **15**, 550 (2014).
54. N. Segata, J. Izard, L. Waldron, D. Gevers, L. Miropolsky, W. S. Garrett, C. Huttenhower, Metagenomic biomarker discovery and explanation. *Genome Biol.* **12**, R60 (2011).
55. S. T. Aspinall, D. N. Hutchinson, New selective medium for isolating *Clostridium difficile* from faeces. *J. Clin. Pathol.* **45**, 812–814 (1992).
56. T. Z. DeSantis, P. Hugenholtz, N. Larsen, M. Rojas, E. L. Brodie, K. Keller, T. Huber, D. Dalevi, P. Hu, G. L. Andersen, Greengenes, a chimera-checked 16S rRNA gene database and workbench compatible with ARB. *Appl. Environ. Microbiol.* **72**, 5069–5072 (2006).
57. A. M. Bolger, M. Lohse, B. Usadel, Trimmomatic: A flexible trimmer for Illumina sequence data. *Bioinformatics* **30**, 2114–2120 (2014).
58. C. A. Smith, E. J. Want, G. O'Maille, R. Abagyan, G. Siuzdak, XCMS: Processing mass spectrometry data for metabolite profiling using nonlinear peak alignment, matching, and identification. *Anal. Chem.* **78**, 779–787 (2006).
59. L. Humbert, M. A. Maubert, C. Wolf, H. Duboc, M. Mahe, D. Farabos, P. Seksik, J. M. Mallet, G. Trugnan, J. Masliah, D. Rainteau, Bile acid profiling in human biological samples: Comparison of extraction procedures and application to normal and cholestatic patients. *J. Chromatogr. B Analyt. Technol. Biomed. Life Sci.* **899**, 135–145 (2012).
60. J. Saric, J. V. Li, Y. Wang, J. Keiser, J. G. Bundy, E. Holmes, J. Utzinger, Metabolic profiling of an *Echinostoma caproni* infection in the mouse for biomarker discovery. *PLOS Negl. Trop. Dis.* **2**, e254 (2008).
61. J. Wu, Y. An, J. Yao, Y. Wang, H. Tang, An optimised sample preparation method for NMR-based faecal metabolomic analysis. *Analyst* **135**, 1023–1030 (2010).
62. Y. Zhao, J. Wu, J. V. Li, N. Y. Zhou, H. Tang, Y. Wang, Gut microbiota composition modifies fecal metabolic profiles in mice. *J. Proteome Res.* **12**, 2987–2999 (2013).

Acknowledgments: We thank C. Salmonson for technical help with the mouse experiments and sample preparation; I. Vuckovic for help with NMR analysis; A. L. Sonenshein for sharing the *C. difficile* Δ prdB mutant; A. Hryckowian and A. S. Akha for assistance with experimental design; J. M. Curry, S. Orwoll, and J. Nielsen for help with figures; S. Johnson for uploading sequencing data to SRA; and K. Zodrow for secretarial assistance. **Funding:** This work was made possible by funding from NIH grant nos. DK100638, DK111850, and DK114007 (to P.C.K.); the Global Probiotics Council (to P.C.K.); Minnesota Partnership for Biotechnology and Genomics (to P.C.K.); the Center for Individualized Medicine, Mayo Clinic (to P.C.K., V.L.H., P.J., N.C., and H.N.); NIDDK grant no. P30 DK 84567 and Administrative and Clinical Cores (to P.C.K., M.G., N.C., G.F., and H.N.); NIH grant no. K23 DK 103911 (to M.G.); Carleton College Summer Science Fellowship (to V.M.R.); NIH grant no. R01 CA179243 (to V.L.H. and N.C.); and the Kolenkow-Reitz Fellowship (to V.M.R.). **Author contributions:** E.J.B., V.L.H., and P.C.K. designed the experiments and the overall data analysis. E.J.B., V.L.H., B.A.S., L.M.T., and W.J.M. performed the mouse experiments and 16S rRNA-based community analysis and prepared samples for RNA-seq and metabolomics. J.C., P.J., V.M.R., L.H., C.R.-M., and N.C. contributed to 16S rRNA, clinical data analysis, and RNA-seq data analysis. S.A.S. and J.L.S. contributed to the metabolomics data analysis. S.K., D.S.P., M.G., R.P., G.F., H.N., and P.C.K. assessed clinical parameters and supervised patient cohort analysis. Y.J.-H. and T.S. assessed histological sections. E.J.B., V.L.H., J.L.S., G.F., and P.C.K. wrote the manuscript with input from the other co-authors. **Competing interests:** R.P. has received funding from BioFire, Check-Points, Curetis, 3M, Merck, Hutchison Biofilm Medical Solutions, Accelerate Diagnostics, Allergan, and The Medicines Company and also serves as a consultant to Curetis, Roche, Qvella, and Diaxonhit. R.P. is a co-inventor on a patent on *Bordetella pertussis/parapertussis* PCR with royalties paid by MOLBIOL GmbH, has a patent on a device/method for sonication with royalties paid by Samsung to Mayo Clinic, and has a patent on an anti-biofilm substance. In addition, R.P. serves on an Actelion data monitoring board, receives travel reimbursement and an editor's stipend from the American Society for Microbiology and Infectious Diseases Society of America, and honoraria from the USMLE, Up-To-Date and the Infectious Diseases Board Review Course. S.K. has received funding from Merck and serves as a consultant to Rebiotix and Summit Pharmaceuticals. D.S.P. consults for Seres Therapeutics, Salix Pharmaceuticals, Cubist Pharmaceuticals, Merck, Janssen, and Otsuka Pharmaceutical. P.C.K., E.J.B., and V.L.H. are co-inventors on a patent no. WO2017053544 A1 (filed 22 September 2016, published 30 March 2017) entitled "Methods and materials for using biomarkers which predict susceptibility to *Clostridium difficile* infection." **Data and materials availability:** 16S rRNA, RNA-seq, and metadata have been deposited in the NCBI Sequence Read Archive (SRA) and are currently available at the following URL: www.ncbi.nlm.nih.gov/sra/SRP075483. The metabolomics data have been uploaded to figshare, and the DOI is 10.6084/m9.figshare.7073294.

Submitted 5 January 2017
Resubmitted 17 November 2017
Accepted 22 March 2018
Published 24 October 2018
10.1126/scitranslmed.aam7019

Citation: E. J. Battaglioli, V. L. Hale, J. Chen, P. Jeraldo, C. Ruiz-Mojica, B. A. Schmidt, V. M. Rekdal, L. M. Till, L. Huq, S. A. Smits, W. J. Moor, Y. Jones-Hall, T. Smyrk, S. Khanna, D. S. Pardi, M. Grover, R. Patel, N. Chia, H. Nelson, J. L. Sonnenburg, G. Farrugia, P. C. Kashyap, *Clostridioides difficile* uses amino acids associated with gut microbial dysbiosis in a subset of patients with diarrhea. *Sci. Transl. Med.* **10**, eaam7019 (2018).

***Clostridioides difficile* uses amino acids associated with gut microbial dysbiosis in a subset of patients with diarrhea**

Eric J. Battaglioli, Vanessa L. Hale, Jun Chen, Patricio Jeraldo, Coral Ruiz-Mojica, Bradley A. Schmidt, Vayu M. Rekdal, Lisa M. Till, Lutfi Huq, Samuel A. Smits, William J. Moor, Yava Jones-Hall, Thomas Smyrk, Sahil Khanna, Darrell S. Pardi, Madhusudan Grover, Robin Patel, Nicholas Chia, Heidi Nelson, Justin L. Sonnenburg, Gianrico Farrugia and Purna C. Kashyap

Sci Transl Med **10**, eaam7019.
DOI: 10.1126/scitranslmed.aam7019

To infect or not to infect?

Our gut harbors a diverse microbial community that efficiently uses nutrients. Battaglioli *et al.* now report that a subset of patients with diarrhea show increased availability of gut amino acids due to deleterious changes in the gut microbiota (dysbiosis). These dysbiotic microbial communities when modeled in germ-free mice exhibited increased susceptibility to *Clostridioides difficile*, a pathogen that uses amino acids as a nutrient source. Prophylactic fecal microbiota transplant from healthy humans to mice with a dysbiotic gut microbiota restored microbial diversity and protected the mice from *C. difficile* infection.

ARTICLE TOOLS	http://stm.sciencemag.org/content/10/464/eaam7019
SUPPLEMENTARY MATERIALS	http://stm.sciencemag.org/content/suppl/2018/10/22/10.464.eaam7019.DC1
RELATED CONTENT	http://stm.sciencemag.org/content/scitransmed/1/6/6ra14.full http://stm.sciencemag.org/content/scitransmed/9/416/eaah6888.full
REFERENCES	This article cites 61 articles, 19 of which you can access for free http://stm.sciencemag.org/content/10/464/eaam7019#BIBL
PERMISSIONS	http://www.sciencemag.org/help/reprints-and-permissions

Use of this article is subject to the [Terms of Service](#)